Published by :
http://www.ijert.org

International Journal of Engineering Research & Technology (IJERT)
ISSN: 2278-0181
Vol. 14 Issue 04, April-2025

Simulation of Stamping Process to Optimize Strength and Cost of B-Pillar of Passenger Vehicle

,

Varsha Turukmane
M. Tech student, Design of Mechanical Systems,
Department of Mechanical Engineering,
Swami Vivekanand College of Engineering, M.P.

Amit Kumar Jha
Senior Manager, Hindustan Aeronautics Limited, Bengaluru, Karnataka

Vishal Wankhade
Assistant Professor, Mechanical Engineering Department,
Swami Vivekanand College of Engineering, Indore, M.P.

Mayank Ladha
Associate Professor HOD Mechanical Engineering Department,
Swami Vivekanand College of Engineering, Indore, M.P.

***Abstract* - A process design technique is presented for the formability assessment of sheet metal stamping parts and feasibility analysis of process conditions. The proposed approach is based on numerical simulation of stamping processes using explicit–incremental and implicit–iterative finite element techniques. The original B-pillar is redesigned to overcome thickness variations during the stamping process by LS-DYNA to meet the strength and durability of the parts.**

***Keywords*- Car; B-pillar; Stamping; Hypermesh; CFD**

I. INTRODUCTION

The body-in-white (BIW) refers to the vehicle body structure at an early stage of production. At this stage, the car's body assembly is complete, but it is devoid of mechanical components, interior trims, and paint. The BIW forms the foundation of a vehicle, providing essential structural integrity and acting as a platform for integrating various systems [1]. The nomenclature of skeleton BIW parts is based on their location in the vehicle, as shown in Fig. 1. Furthermore, as from Fig. 1, the components of the vehicle collectively ensure vehicle safety, rigidity, and performance.

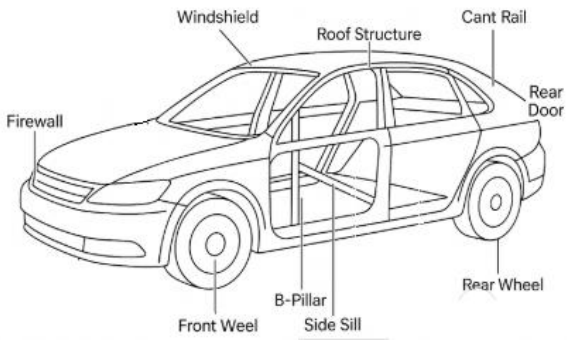

Figure1: Nomenclature of structural parts of BIW

From Fig. 1, the B-pillar serves as a primary load-bearing structure during side impacts and rollovers, ensuring passenger safety and maintaining cabin integrity [1]. The B-pillar acts as a critical load path by transferring forces from the roof to the side sills and floor pan. In addition, the connection of the B-pillar to multiple structural components adds lateral and vertical stability to ensure minimal intrusion into the cabin during rollovers, safeguarding occupants seated near the pillar.

Therefore, the strength of the B-pillar directly influences the overall crashworthiness of the vehicle. Typically, B-pillars are made of ultra-high-strength steels (UHSS) or advanced composites for optimal strength and weight balance to ensure that vehicles meet stringent safety standards, enhancing consumer trust and marketability.

The complex components, like the B-pillar in the automobile industry, used different manufacturing processes for production. In that, stamping is a highly versatile and widely used manufacturing process in the automotive industry, particularly for the production of complex metal components such as the B-pillar [2-3]. The process of stamping involves shaping flat metal sheets into desired geometries using dies and presses under high pressure, as shown in Fig. 2.

(This work is licensed under a Creative Commons Attribution 4.0 International License.)

International Journal of Engineering Research & Technology (IJERT)
ISSN: 2278-0181
Vol. 14 Issue 04, April-2025

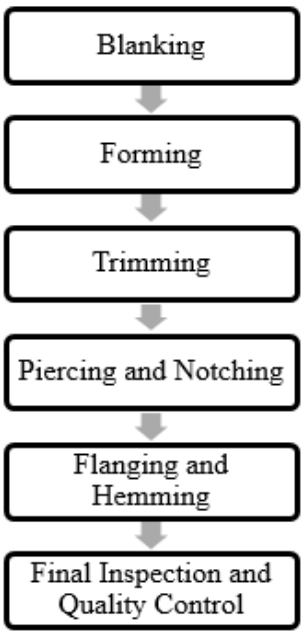

Figure 2: Stamping Process

- Blanking

Purpose: Produces the raw metal sheet, or blank, from larger sheets or coils.

Process: A cutting operation where a die is used to shear the material into a rough shape that matches the final component's outline.

Significance: Ensures minimal material wastage and prepares the blank for subsequent forming operations.

- Forming

Purpose: Shapes the blank into a three-dimensional geometry.

Process: The blank is placed between a punch and a die, and high force is applied to deform the material plastically.

Significance: Forms the preliminary shape of the component while avoiding defects like tearing or wrinkling.

- Trimming

Purpose: Removes excess material from the formed component.

Process: A cutting operation performed using secondary dies to achieve precise dimensions.

Significance: Ensures the final shape meets the required specifications for assembly.

- Piercing and Notching

Purpose: Creates holes or slots in the component.

Process: Uses specially designed punches and dies to remove material in a controlled manner.

Significance: Essential for features such as mounting points or openings for other vehicle systems.

- Flanging and Hemming

Flanging: Bends the edges of the component for assembly or reinforcement.

Hemming: Folds the edges of the sheet metal over itself to create a smooth edge or join multiple components.

- Final Inspection and Quality Control

Purpose: Ensures the stamped part meets dimensional tolerances and quality standards.

Techniques: Visual inspection, dimensional measurement, and simulation-based validation (e.g., finite element analysis).

The stamping process is used in manufacturing for high efficiency, precision, cost-effectiveness, and versatility. But stamping has many challenges during manufacturing, such as material thinning, wrinkling and tearing, elastic recovery after forming, and tool wear, respectively [2].
Therefore, role of simulation in stamping is essential. Different methods area discussed:

Predictive Modeling: Tools like LS-DYNA simulate material behavior and identify potential defects like thinning, tearing, and wrinkling.

Process Optimization: Adjusts parameters such as die design, material thickness, and lubrication to enhance efficiency and product quality.

Cost Savings: Reduces trial-and-error in the physical prototyping phase.
The stamping process, aided by advanced simulation tools, forms the backbone of modern automotive manufacturing, ensuring high-quality and safety-compliant components at scale.

II. LITERATURE REVIEW

The stamping process for different parts of automobiles, preparation, and finite element modeling with analysis are studied by various authors.
A process design technique is presented for the formability assessment of sheet metal stamping parts and feasibility analysis of process conditions. The proposed approach is based on numerical simulation of stamping processes using explicit–incremental and implicit–iterative finite element techniques. The authors validated the present method by springback predictions for an engine suspension bracket made of high-strength steel. The predicted part shapes closely matched CMM measurements, confirming the method's reliability [4]. The drawing process of a fender was simulated by finite element analysis software DYNAFORM. An orthogonal test was also designed to optimize parameters such as blank holder force, model

(This work is licensed under a Creative Commons Attribution 4.0 International License.)

International Journal of Engineering Research & Technology (IJERT)
ISSN: 2278-0181
Vol. 14 Issue 04, April-2025

clearance, friction coefficient, and die radius. In addition, the experimental results confirmed that the optimal parameter combination improved fender performance, enhancing manufacturability and stability [5]. The authors integrated finite element analysis (FEA) with multiple regression analysis to optimize stamping parameters and minimize sheet thinning. Stamping involves complex tensile and compressive stresses, which may cause thinning or wrinkling. FEA predicts stress distributions, while regression analysis establishes relationships between process parameters and responses. Validation through experimental production showed reduced thinning, emphasizing the approach's capability to improve manufacturing quality [6]. The author described the integration of finite element analysis with mesh morphing and response surface optimization to create a user-friendly software tool. The workflow, implemented via Hyper-Form, minimizes defects in stamped parts during both product development and process design stages. Application results demonstrated improved efficiency and quality in stamping simulations [7]. Accurate springback prediction in sheet metal deformation is critical for tooling design, especially for high-strength steels. The author focused on the above and studied a rate-independent cyclic plasticity model in LS-Dyna for high simulation accuracy. Simulations of a dual-phase steel automotive part showed better performance in springback prediction compared to isotropic plasticity. Experimental validation via surface scanning proved the superiority of the proposed model in stamping applications [8]. The author explained hot stamping processes and accurate modeling by finite element analysis (FEA) to predict component quality. This study presents a software-agnostic platform for cloud-based FEA involving pre-simulation, simulation, and post-simulation stages. Flow stress, material properties, and interfacial heat transfer coefficients were predicted using model-driven modules. Application of two hot stamping technologies showed error margins below 10%, demonstrating the platform's effectiveness in thermomechanical characteristic evaluation [9]. The author discussed the stamping process of car radiator upper beams, focusing on their complex shapes and deformation challenges. Simulation analysis optimized parameters like blank holder force and die radius to enhance the process. Results showed improved manufacturing efficiency and better part quality. This study offers insights into the effective design and simulation of complex automotive components [10]. The author examined roof crush performance by Finite Element Analysis (FEA) as per FMVSS 216 standards. The study systematically develops an optimal combination of computational parameters to closely align simulation results with physical test outcomes. This work highlights the importance of accurate modeling techniques to enhance roof design and safety [11]. Rollover accidents account for a significant number of vehicular fatalities annually, emphasizing the importance of robust roof design. The author focused on the above and studied roof strength using FEA tools like LS-DYNA. The study explored materials like composites to enhance roof strength while minimizing sheet metal thickness. The results were validated by simulation data against regulatory benchmarks, presenting a methodical approach for roof material optimization [12]. The author studied static FMVSS 216 roof crush tests with dynamic inverted drop tests, highlighting the latter's realism in simulating real-world rollover impacts. Using FEA models of vehicles like the Ford Fiesta and Renault Clio, the research identifies critical orientations causing maximum roof deformation. Results indicate that dynamic tests better represent structural vulnerabilities, revealing weak roof components inadequately addressed by static tests. The present results revealed the necessity of dynamic testing in conjunction with computational modeling for robust roof evaluations [13].

III. MATERIALS AND METHODS

Material behavior in the stress analysis is studied by stress-strain curves to understand the behavior of materials under load [1] [14-15]. The two main types of stress-strain curves used in engineering are engineering stress-strain curves and true stress-strain curves. Both curves describe the relationship between the stress applied to a material and its resulting strain (deformation), but they differ in how they account for changes in the material's geometry during deformation, as shown in Fig. 3.

- Engineering Stress-Strain Curve

Engineering Stress (σ) is defined as the force (F) applied to the material divided by the original cross-sectional area (A_0):

$$\sigma = \frac{A}{F}$$

Engineering Strain **(ε)** is defined as the change in length (ΔL) divided by the original length (L_0):

$$\varepsilon = \frac{L0}{L}$$

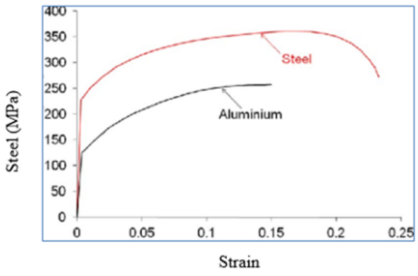

Figure 3: S-300 steel engineering stress-strain curve Vs aluminum alloys stress- strain curve

- True Stress-Strain Curve

The true stress-strain curve, on the other hand, accounts for the actual changes in the material's geometry during deformation. It provides a more accurate representation of the material's behavior, particularly under large strains (such as in plastic deformation).

(This work is licensed under a Creative Commons Attribution 4.0 International License.)

International Journal of Engineering Research & Technology (IJERT)
ISSN: 2278-0181
Vol. 14 Issue 04, April-2025

True Stress (σ_t) is defined as the force (F) applied to the material divided by the actual (instantaneous) cross-sectional area (A):

$$\sigma t = \frac{A}{F}$$

True Strain **(ε_t)** is defined as the natural logarithm of the ratio of the instantaneous length (L) to the original length (L_0):

$$\varepsilon t = \ln\left(\frac{L0}{L}\right)$$

Since true stress takes the change in area into account and true strain accounts for the continuous change in length, the true stress-strain curve provides a more precise description of the material's behavior under load, especially during plastic deformation.

- Finite Element Analysis (FEA)

FEA simulates the behavior of materials and structures under various loading conditions. For accurate results, FEA requires true stress-strain data rather than engineering stress-strain data for the following reasons:

- ➢ Accurate Prediction of Material Behavior
- ➢ Nonlinear Deformation
- ➢ Accurate Failure Predictions

- Method to convert Engineering Stress-Strain Curve to True Stress-Strain Curve

Converting the engineering stress-strain curve to the true stress-strain curve is essential when performing FEA simulations, especially for materials that undergo significant plastic deformation. The conversion can be done using the following relationships [1][14-15]:
True Stress from Engineering Stress

$$\sigma t = \sigma(1 + \varepsilon)$$

where,

σt is the true stress, σ is the engineering stress, and ε is the engineering strain.

True Strain from Engineering Strain

$$\varepsilon t = ln(1 + \varepsilon)$$

where,

εt is the true strain and ε is the engineering strain.

These equations are valid during plastic deformation, particularly after yielding, where the material undergoes necking and significant changes in its geometry. The true stress-strain curve typically rises more steeply than the engineering stress-strain curve during plastic deformation, as the material hardens and its cross-sectional area decreases.

Material used in stamping process is given in Table 1.

Table 1: Material properties of S-300

Engineering Strain (ε)	True Strain (ε_t)	Engineering Stress (σ_e) [MPa]	True Stress (σ_t) [MPa]
0.0001	0.0001	21	21
0.001	0.00099	63	63
0.00143	0.00143	300	300
0.01	0.00995	350	377.8
0.05	0.04879	400	472.6
0.1	0.09531	450	567.3
0.15	0.1398	500	656.4
0.2	0.1823	550	735.5

Apart from Table 1 properties, elastic modulus (210 GPa) and Poisson's ratio (0.3) are considered.

- Stamping process

The stamping process is a widely used manufacturing technique for shaping and cutting metal sheets into specific forms through the use of a die and press. This process is prevalent in industries like automotive, aerospace, and electronics, where it is used to create components such as body panels, connectors, and structural parts. The procedure involves several stages that apply high pressure to deform metal sheets into the desired shape, with variations based on the complexity of the part being manufactured. Below is an outline of the general stamping process.

- ➢ Material Selection

Materials commonly used include Steel (including mild, high-strength, and stainless steel), Aluminum alloys, Copper alloys, Brass and Titanium (for specialized applications). The choice of material depends on factors such as the part's required mechanical properties, formability, and strength, and it plays a crucial role in determining the stamping process parameters.

- ➢ Blanking

The stamping process typically begins with blanking, where a flat sheet of metal is cut into a "blank" — the raw material that will be further shaped.

- ➢ Die Setup and Design

A die is composed of two key components: the punch (which shapes the material) and the die cavity (which holds the material). The design of the die is essential for producing parts with the correct dimensions and for maintaining tool durability. Key steps in die setup are given below as shown in Fig. 4.

- ❖ Selection of die materials
- ❖ Die design
- ❖ Tooling setup

(This work is licensed under a Creative Commons Attribution 4.0 International License.)

International Journal of Engineering Research & Technology (IJERT)
ISSN: 2278-0181
Vol. 14 Issue 04, April-2025

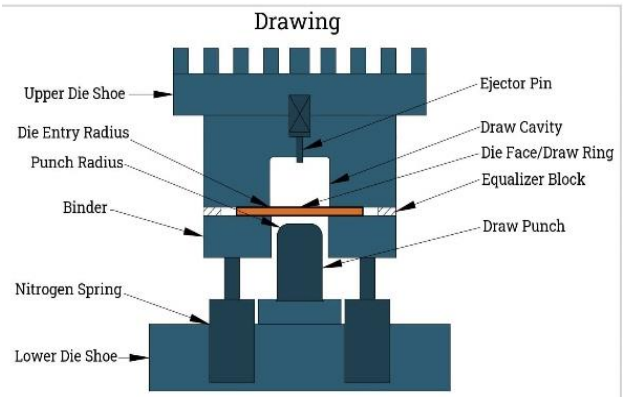

Figure 4. Die setup

- Press Machine Operation

The press machine applies force to the die to perform the shaping. Depending on the press type (mechanical or hydraulic), the machine's force capacity can vary. The press moves the punch into the die, pressing the metal into the required shape. Several operations like blanking, punching, etc. are selected based on the specific design and complexity of the part.

- Deformation and Material Shaping

During the press operation, the metal undergoes deformation, either elastic or plastic, depending on the amount of force applied. For complex shapes, like those used in automotive body panels, processes like deep drawing or stretch forming are employed to transform the flat material into 3D structures.

- Trimming and Finishing

After forming, trimming is used to remove excess material, often called flash, around the edges of the part. This ensures that the part adheres to the final specifications.

- Material selection for the B-pillar

The material used for the B-pillar is critical since it has a direct impact on the vehicle's structural integrity and safety. The B-pillar is a vital component of the vehicle's safety system, providing strength to the cabin during side-impact collisions. Steel and aluminium alloys are options to maintain the required strength for crashworthiness.

- Methodology for Simulation of Stamping Process by LS-DYNA and Stress and Strain by OptiStruct - B-Pillar

The simulation of the stamping process for the B-pillar and the subsequent calculation of stress and strain are crucial steps in optimizing automotive component design. The B-pillar is a key structural component that provides support for the vehicle's roof and contributes to passenger safety during side-impact and rollover events [3] [7] [16].
The approach, incorporating material modeling, process simulation, and optimization are

- Simulation of the Stamping Process Using LS-DYNA
  - Geometry Definition

Create the B-pillar geometry based on the design specifications.

  - Material Selection

Define the material properties (young's modulus, poison's ratio, density) of the B-pillar of the material (e.g., high-strength steel, aluminum alloys).

  - Mesh Generation

Create a finite element mesh for the B-pillar geometry. Mesh refinement is essential to capture details accurately during the stamping process. Hexahedral or tetrahedral elements for the body of the B-pillar. Shell elements for thin parts like the flanges, which are commonly used in sheet metal forming simulations. Apply mesh refinement in areas where high deformation or stress is expected.

  - Boundary Conditions and Initial Setup

Apply boundary conditions that simulate the real-life conditions of the stamping process. In the present, constraints at the die surface to simulate the press tool. Apply initial velocity or force at specific locations to represent the movement of the punch or die during stamping.

Define contact definitions between the B-pillar sheet and the die surfaces. This step ensures that the correct interactions between the part and the die are accounted for during the stamping process.

  - Solving the Stamping Process Using LS-DYNA

The stamping process is simulated in time steps using explicit dynamic analysis in LS-DYNA. The software solves the equations of motion for the B-pillar under the applied loads and boundary conditions.

  - Post-Processing and Results Analysis in LS-DYNA

After the simulation, LS-DYNA provides the strain and stress distribution across the B-pillar.

- Calculation of Stress and Strain of B-Pillar Using OptiStruct

After the stamping process, OptiStruct is used to calculate the stress and strain distribution of the final B-pillar geometry. OptiStruct is an advanced solver for structural analysis and optimization, widely used for assessing the performance of components under various loading conditions.

  - Geometry

Import the B-pillar geometry from LS-DYNA (if using a unified simulation) or from a CAD model.

  - Mesh

Generate a finite element mesh for the B-pillar, with appropriate mesh density in areas where high stress or deformation is expected.

(This work is licensed under a Creative Commons Attribution 4.0 International License.)

International Journal of Engineering Research & Technology (IJERT)
ISSN: 2278-0181
Vol. 14 Issue 04, April-2025

➢ Material Modeling

Define the material properties in OptiStruct, including elastic modulus, yield strength, Poisson's ratio, and hardening behavior. Use true stress-strain curves from LS-DYNA to ensure accurate material behavior under large deformations and loading conditions.

➢ Boundary Conditions and Loading

Apply boundary conditions such as fixed supports or constrained nodes to represent the mounting points and load application in a vehicle. Apply relevant loads to simulate operational conditions of the B-pillar, including side impact forces, roof crush forces, or structural support during vehicle operation.

➢ Stress and Strain Calculation

Use linear static analysis to calculate the response of the B-pillar under simple loading conditions (e.g., constant forces or displacements). Perform nonlinear static analysis to account for plastic deformation, large displacements, and material yielding under more complex loads. OptiStruct output the stress and strain distribution across the B-pillar, helping to identify critical regions that may require design modifications. The von Mises stress is typically used to assess whether the material exceeds its yield strength, while strain helps in understanding material deformation and plastic flow.

➢ Post-Processing and Result Interpretation

After the simulation, OptiStruct provides detailed plots of stress and strain, which can be analyzed to identify failure-prone regions or areas where further strengthening is required.

Methodology process chart of the above is shown in Fig. 5.

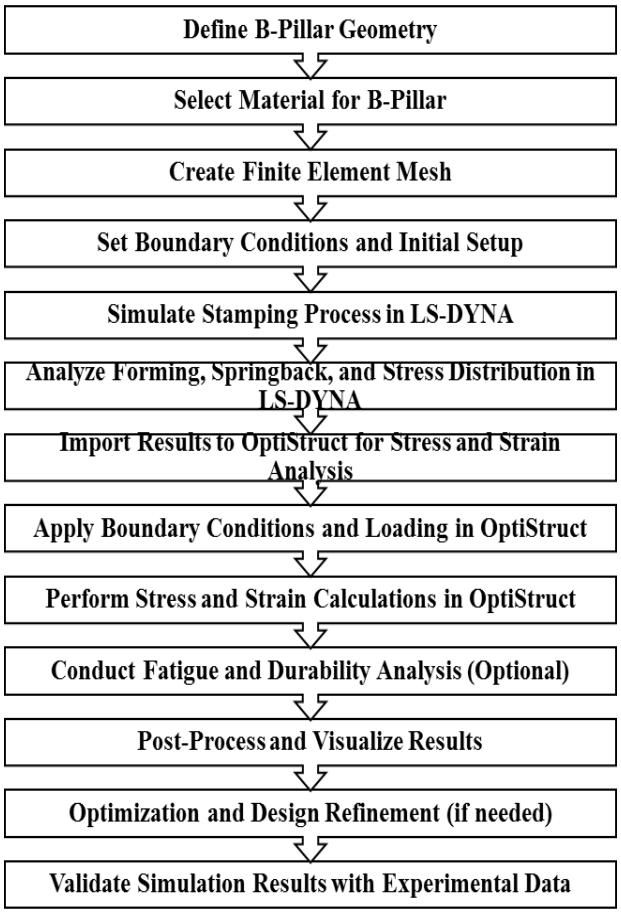

Figure 5. Methodology process chart

IV. RESULTS AND DISCUSSIONS

- FEA of stamping process of B-pillar of a car

Modeling a simplified design in Creo Parametric, taking into account that this has to be manufactured using a stamping process, thus removing complications in CAD, is shown in Fig. 6. A zoomed view of the meshing of the B-pillar is shown in Fig. 7. Meshing of the B-pillar in Hypermesh software with a 1 mm mesh size of the shell element and assigned a thickness of 3 mm as measured from the original B-pillar. Quality of elements details are given in Table 2.

Static simulation to benchmark the strength of the original B-pillar is explained in the present study. The focus is on evaluating the deformation and strength of the B-pillar under a specified load, rather than simulating roof crush. To do so, the B-pillar will be fixed at one end, simulating the attachment to the vehicle body, while a force of 300 kg will be applied at a 45-degree angle from the other end, as shown in Fig. 8. The force is considered in the finite element model of the B-pillar, both in its original, undeformed state and after undergoing the stamping process.

(This work is licensed under a Creative Commons Attribution 4.0 International License.)

Published by :
http://www.ijert.org

International Journal of Engineering Research & Technology (IJERT)
ISSN: 2278-0181
Vol. 14 Issue 04, April-2025

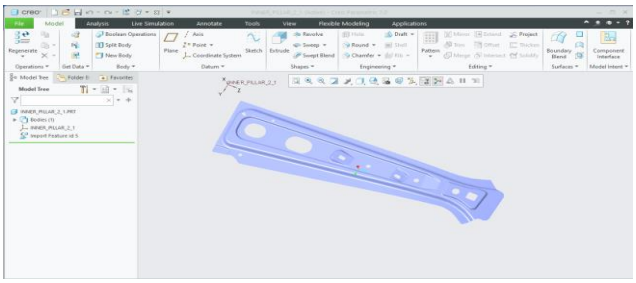

Figure 6. Geometry of B-pillar

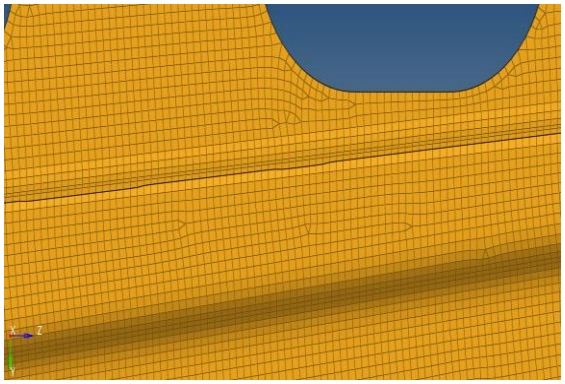

Figure 7. Zoom view of meshed B-pillar

Table 2: Quality of elements

MESH PARAMETER	WROST ELEMENT	ACCEPTABLE LIMIT
WARPAGE	3.5	<15
SKEW	51.05	<60
ASPACT	12.2	<15
JACOBIAN	0.56	>0.5

The simulation will calculate the deformation values, as shown in Fig. 9, of both the original B-pillar and the one formed through stamping, with a particular emphasis on assessing how the forming process influences the pillar's structural integrity.

By comparing the deformation results and the overall strength of the two models, the study will provide insights into how the stamping process affects the B-pillar's performance under load. The deformation will be analyzed in terms of displacement and stress distribution, and the strength will be evaluated based on the material's yield strength, stress concentration areas, and failure points. The following comparison will help assess whether the forming process strengthens or weakens the B-pillar, offering valuable data for design optimization.

Figure 8: Boundary condition for benchmarking

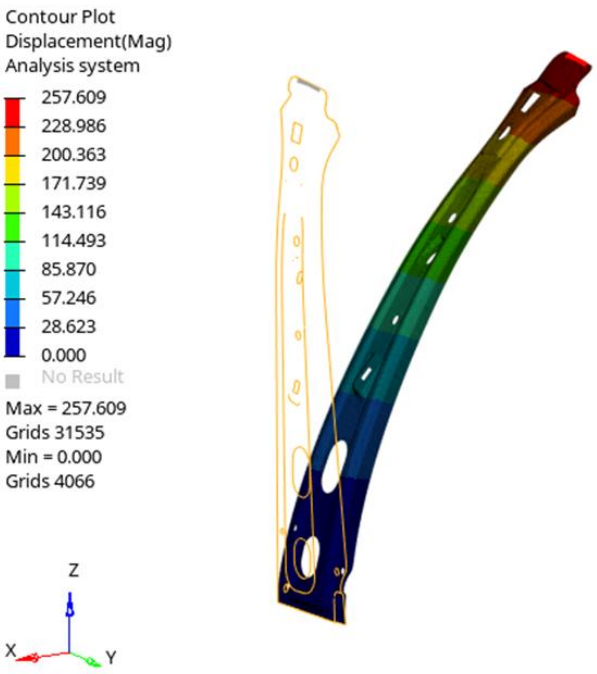

Figure 9: Displacement plot

The setup for the simulation of the stamping process is shown in Fig. 10.

(This work is licensed under a Creative Commons Attribution 4.0 International License.)

International Journal of Engineering Research & Technology (IJERT)
ISSN: 2278-0181
Vol. 14 Issue 04, April-2025

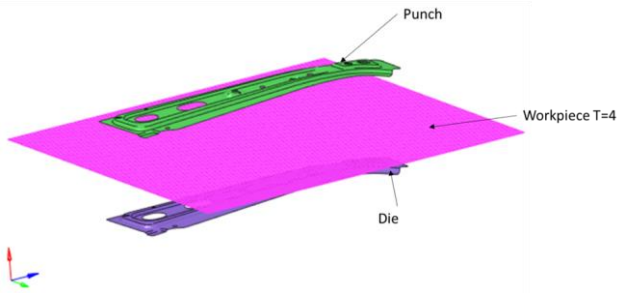

Figure 10.Setup of stamping process

For the simulation of the punching process in LS-DYNA, a simple rectangular workpiece is created using the previously defined material properties. The setup includes a rigid die and punch, with the workpiece placed between them. The punch is assigned a velocity, which is directed toward the rigid die. As the punch moves toward the die, it applies a compressive force on the workpiece, causing it to deform and take the shape of the die impression. This process simulates the material flow as the punch forms the workpiece. Once the punch has completed its motion, post-processing is performed on the workpiece to analyze various parameters, including the material thickness distribution and the overall quality of the B-pillar. Assessing the effectiveness of the stamping process by examining the changes in material thickness and identifying any inconsistencies or weak points, such as areas with excessive thinning or irregular stress distribution. This simulation provides a comprehensive understanding of the deformation behavior, material properties, and the potential for optimizing the B-pillar design for strength and durability. Results from stamping FEA are shown in Fig. 11 and Fig. 12, respectively.

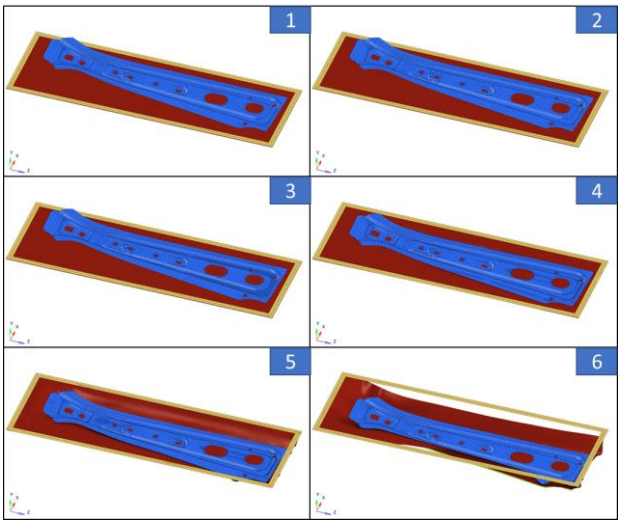

Figure 11: Animation Frames

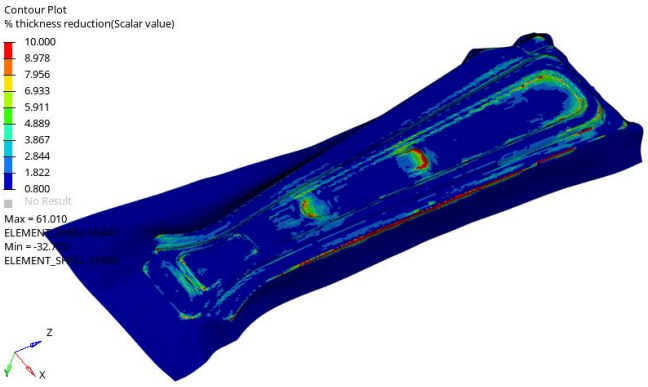

Figure 12: % Thickness reduction due to stamping

Contour analysis of the forming process is explained by Fig. 12.
Red Areas Indication: Areas marked in red represent regions with a thickness reduction of more than 60%.
Impact on Strength: Such a significant reduction in thickness negatively impacts the strength of the B-pillar.
Compensation Strategy: To address that a workpiece with a higher initial thickness, such as 4 mm, can be considered to mitigate strength loss.

- Structural analysis using OptiStruct of the B-pillar

The original B-pillar design had a uniform thickness of 3 mm. This was chosen as a cost-effective option for manufacturing. However, to assess the feasibility of producing the B-pillar using the stamping process, the simulations was conducted using LS-DYNA.
LS-DYNA results are imported in OptiStruct. Further, simplified thickness plots and comparisons of displacements are discussed as shown in Fig. 14 and Fig. 15, respectively.
The comparison shows that the displacement variation from the stamping process to the analysis is within 6 %.

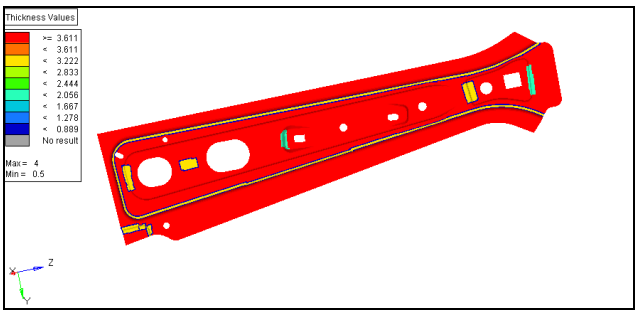

Figure 14: Simplified thickness plot

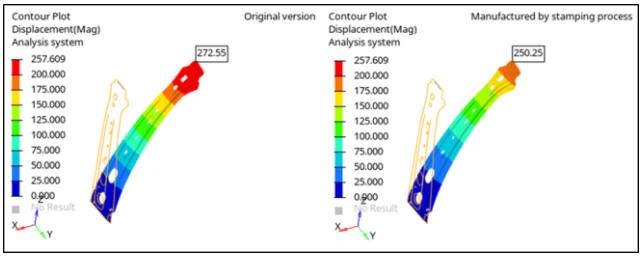

Figure 15: Comparison of displacement results (original Vs manufactured)

(This work is licensed under a Creative Commons Attribution 4.0 International License.)

International Journal of Engineering Research & Technology (IJERT)
ISSN: 2278-0181
Vol. 14 Issue 04, April-2025

The simulations revealed that the stamping process results in thickness variations across the workpiece. Specifically, certain areas of the final product experience significant thinning, which compromises the structural integrity of the B-pillar. To address this issue and compensate for the reduction in thickness caused by the stamping process, a workpiece with an initial thickness of 4 mm was used instead of 3 mm. This adjustment ensures that the final product meets the required strength and durability standards while maintaining the feasibility of the manufacturing process.

V. CONCLUSION

The original B-pillar was designed with a uniform thickness of 3 mm to optimize manufacturing costs. LS-DYNA simulations revealed that the stamping process results in thickness variations, with certain areas experiencing significant thinning. The reduction in thickness compromises the structural integrity of the B-pillar.

Therefore, an initial workpiece thickness of 4 mm was proposed instead of 3 mm. The following selection in thickness ensures that the final product meets strength and durability requirements while maintaining manufacturing feasibility.

ACKNOWLEDGEMENT

I am thankful to my friends for their kind support.

REFERENCES

[1] P. Hu, L. Ying, B. He, Hot stamping advanced manufacturing technology of lightweight car body, Springer Science Press Beijing, ISSB 978-981-10-2401-6, doi.10.1007/978-981-10-2401-6, 2017.

[2] Y.Lim, R.Venugopal, et al, Process control for sheet -metal stamping, Advances in Industrial Control, Springer-Verlag London, ISSB 978-1-4471-6284-1, doi. 10.1007/978-1-4471-6284-1, 2014.

[3] S. Verma, M. Lodha, M. Sharma, R. Joshi, “CFD modelling calculation and simulation of bus,” International Research Jounral of Engineering and Technology 10(6) :e-ISSN:2395-0056, p-ISSN:2395-0072, 2023.

[4] M. Firat,O. H. Mete, et al “Stamping process design using FEA in conjunction with orthogonal regression,” Finite Elements in Analysis and Design 46: 992–1000,2010.

[5] P. Wu, Y. Wang, P. Wan, “Study on Simulation of Stamping Process and Optimization of Process Parameters of Fender,” Advances in Materials Science and Engineering, pages 1-9, 4081632, doi.org/10.1155/2019/4081632, 2019.

[6] T. Y. Badgujar, V. P. Wani, “Stamping Process Parameter Optimization with Multiple Regression Analysis Approach,” Materials Today: Proceedings 5: 4498–4507, 2018.

[7] S. Roy, C. Sharma, H. Palaniswamy, “Seamless Integration of Stamping Simulation with Product and Process Optimization,” International Deep Draw Research Group (IDDRG), 2015.

[8] M. Firat,E. Karadeniz, et al “Improving the Accuracy of Stamping Analyses Including Springback Deformations,” Journal of Materials Engineering and Performance, 22:332–337, doi: 10.1007/s11665-012-0257-5, 2013.

[9] M. Zhu,Y. C. Lim, et al “Cloud FEA of hot stamping processes using a software agnostic platform,” The International Journal of Advanced Manufacturing Technology, 112:3445–3458, 2021.

[10] J. Tan, Advances in mechanical design, Proceedings of the 2019 International Conference on mechanical design (2019 ICMD), Springer Nature Singapore Pte Ltd, 77,ISSB 978-981-32-9941-2, doi.10.1007/978-981-32-9941-2, 2020.

[11] N. Narayana, "Accurate FEA Predictions for Roof Crush Performance of Automotive Structures," SAE Technical Paper 2011-01-1063, doi.10.4271/2011-01-1063, 2011.

[12] V. Pathak, A. Kutimbale, et al, “Design Optimization of Vehicle Body Structure against Roof Crush as per FMVSS 216 Using Finite Element Analysis (FEA),” Research Journal of Engineering Sciences, 4(5): 1-7, 2015.

[13] M. Mao, E. C. Chirwa, W. Wang, “Assessment of Vehicle Roof Crush Test Protocols Using FE Models: Inverted Drop Tests versus updated FMVSS No. 216,” International Journal of Crashworthiness, 11(1):49-63, doi.10.1533/ijcr.2005.0383, 2006.

[14] M. C. Y. Niu, Airframe stress analysis and sizing, Hong Kong Conmmilit press LTD, 2nd edition, 1999.

[15] S. Kumar, A. K. Jha, G R Kesheorey, “Design and Fatigue Analysis of a Typical Aircraft Wing fuselage Lug attachment structure,” International Research Jounral of Engineering and Technology 10 (1):e ISSN:23950056, p-ISSN:23950072, 2023.

[16] N. Nahar, A. K. Jha, M. Sharma, R. Joshi, “Aerodynamic analysis of ramp type vortex generator on NACA 2215 airfoil,” International Research Jounral of Engineering and Technology 10(6) :e-ISSN:2395-0056, p-ISSN:2395-0072, 2023.

(This work is licensed under a Creative Commons Attribution 4.0 International License.)